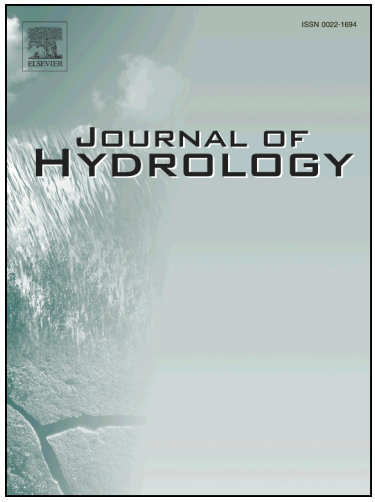

Research papers

Response of leaf stable carbon isotope composition to temporal and spatial variabilities of aridity index on two opposite hillslopes in a native vegetated catchment

Xiang Xu, Huade Guan, Grzegorz Skrzypek, Craig T. Simmons

PII: S0022-1694(17)30391-8
DOI: http://dx.doi.org/10.1016/j.jhydrol.2017.05.062
Reference: HYDROL 22053

To appear in: *Journal of Hydrology*

Received Date: 6 September 2016
Revised Date: 30 May 2017
Accepted Date: 31 May 2017

Please cite this article as: Xu, X., Guan, H., Skrzypek, G., Simmons, C.T., Response of leaf stable carbon isotope composition to temporal and spatial variabilities of aridity index on two opposite hillslopes in a native vegetated catchment, *Journal of Hydrology* (2017), doi: http://dx.doi.org/10.1016/j.jhydrol.2017.05.062

Response of leaf stable carbon isotope composition to temporal and spatial variabilities of aridity index on two opposite hillslopes in a native vegetated catchment

Xiang Xu[1,2,3]* Huade Guan[1,2] Grzegorz Skrzypek[4,1] Craig T. Simmons[1,2]

1. School of the Environment, Flinders University of South Australia.
2. National Centre for Groundwater Research and Training, Flinders University of South Australia.
3. Key Laboratory of Western China's Environmental Systems (Ministry of Education), College of Earth and Environmental Sciences, Lanzhou University, Lanzhou 730000, China.
4. West Australian Biogeochemistry Centre, School of Biological Sciences, The University of Western Australia.

*Corresponding author and address: X. Xu

School of the Environment

Flinders University of South Australia

GPO Box 2100

Adelaide 5001

South Australia

Phone No: +61 8 82012976

E-mail: xxiang@lzu.edu.cn

Abstract

The stable carbon isotope composition ($\delta^{13}C$) has been demonstrated to be a useful indicator of environmental conditions occurring during plant growth. Previous studies suggest that tree leaf $\delta^{13}C$ is correlated with mean annual precipitation (MAP) over a broad range of climates with precipitation between 100 to 2000 mm/year. However, this relationship confirmed at the large scale may not be present at the local scale with complex terrain where factors other than precipitation may lead to additional variability in plant water stress.

In this study, we investigated $\delta^{13}C$ of tree leaves in a native vegetation catchment over a local gradient of hydro-climatic conditions induced by two hillslopes with opposite aspects. Significant seasonal variations, calculated as a difference between the maximum and minimum $\delta^{13}C$ values for each tree, were observed for two species, up to 1.9‰ for *Eucalyptus* (*E.*) *paniculata*, and up to 2.7‰ for *Acacia* (*A.*) *pycnantha* on the north-facing slope (NFS). Also the mean $\delta^{13}C$ values calculated from all investigated trees of each hillslope were significantly different and leaf $\delta^{13}C$ on the NFS was higher by 1.4 ± 0.5‰ than that on the south-facing slope (SFS). These results cannot be explained by the negligible difference in precipitation between the two hillslopes located just 200 m apart. The correlation coefficients between the $\delta^{13}C$ of *E.* tree leaves and the integrated aridity index (AI) were statistically significant for temporal observations on the NFS (R^2 0.18 - 0.44, p-value 0.00 - 0.06), and spatial observations (R^2 = 0.35, p-value 0.05) at the end of the dry

season. These results suggest that AI as a measure of plant water stress is better associated with leaf $\delta^{13}C$ than precipitation. Therefore, leaf $\delta^{13}C$ value can be used as a valuable proxy for plant water stress across the landscape in both time and space.

Keywords: leaf $\delta^{13}C$; aridity index; hillslopes; water stress; South Australia

1. Introduction

Temperature, solar irradiance, and water in different climatic zones impose varying limitations on vegetation growth, and thus drive vegetation distribution globally (Nemani, et al., 2003). In comparison to solar radiation and temperature, water availability is much more dynamic, and temporarily and spatially variable (Good and Caylor, 2011; Nemani, et al., 2003; Vicente-Serrano et al., 2013). In a water limited environment, extreme droughts may even lead to changes in ecosystem structures (McDowell et al., 2008). Complex terrain, redistributing water and altering energy inputs, can affect the local distribution of tree species (Gutiérrez-Jurado, et al., 2013). Local hydrogeologcial and soil conditions, such as root-zone thickness, soil texture, distance to streams, and depth to groundwater table can result in different levels of water stress on vegetation (Dawson and Ehleringer, 1991; Liu et al., 2017; Lloret et al., 2003; Lubczynski, 2009; Sardans and Peñuelas, 2013).

Quantification of the plant water stress is necessary to improve our understanding of tree resilience to various changes of environmental conditions. However, conventional physiological methods of water stress monitoring, such as photosynthesis carbon assimilation and soil moisture observations, usually offer snap-shot information at the time of measurement only. They are neither applicable for investigating the cumulative water stress from seasonal to multi-seasonal scales, nor for developing the relationship between the stable carbon isotope of tree rings and climate for paleoclimate reconstruction.

Conversely, the stable carbon isotope ratio $^{13}C/^{12}C$ of leaves (expressed as leaf $\delta^{13}C$) has been demonstrated to be a useful indicator of environmental conditions during the growth periods (Farquhar and Sharkey, 1982). During photosynthesis, the overall carbon isotope fractionation is primarily controlled by the stomata conductance and associated diffusion of the atmospheric CO_2 to leaves (O'Leary, 1981; Hesterberg and Siegenthaler, 1991), and the carboxylation during the CO_2 fixation (e.g. Schmidt et al., 1978; Guy et al., 1987). These two processes are related to the negative gradient of intercellular CO_2 molar concentration and CO_2 absorption through regulation of the stomatal aperture. The status of stomatal aperture also controls water loss through transpiration. Thus, environmental factors (solar irradiance, temperature, vapour pressure deficit, and root zone soil moisture) which influence the stomatal conductance (Jarvis, 1976; Wang et al., 2014) will impact both CO_2 and water vapour exchange, and cause the stable carbon isotope fractionation between the atmospheric CO_2 and produced biomass (Farquhar et al., 1989).

Individual environmental factors such as solar irradiance (e.g. Pearcy, 1988), temperature (e.g. Evans and von Caemmerer, 2013; Skrzypek et al., 2007), and soil moisture factors (e.g. salinity, (van Groenigen and Kessel, 2002)) have been reported influencing leaf $\delta^{13}C$. Each of these factors could potentially be an overwhelming driver of the stable carbon isotope fractionation in certain environments. Some of these factors such as salinity and nutrient stresses are generally spatially restricted but less temporarily variable. Other climate-related factors, such as temperature, solar

irradiance and water availability, are more common drivers. The influence of temperature on leaf $\delta^{13}C$ has not been studied widely. The most consistent pattern was observed in lower plants with less complicated metabolism such as mosses (Skrzypek et al., 2007). Evans and von Caemmerer (2013) showed that when leaf temperature increases from 15 to 40°C, carbon fractionation associated with photorespiration decreases by 1.6‰ in tobacco. Other diverse values -1 to -2.4‰ /°C were also reported for various environments and species (Skrzypek et al., 2013) with different factors at different temperatures (Smith et al., 1976; Troughton and Card, 1975).

Therefore, leaf $\delta^{13}C$ can be potentially used as an indicator of the lumped effect of environmental stress on stomatal conductance. Such a lump effect on stomatal conductance has been commonly applied in transpiration modelling (e.g., Wang et al. 2016). In water limited environment, water stress from limited water supply (e.g., soil moisture) on one hand, and excess atmospheric demand (i.e., potential evapotranspiration, PET) on the other hand, is the most limiting factor for plant physiological activities (Yang et al., 2013; Liu et al., 2017). Local availability of soil water (Farquhar and Sharkey, 1982) and potential evapotranspiration (PET) have been shown commonly influencing leaf $\delta^{13}C$ (Cernusak et al., 2013; O'Leary et al., 1981).

Previous large-scale studies (e.g. Diefendorf et al., 2010; Miller et al., 2001; Schulze et al., 1998), conducted over a broad range of climatic conditions, have shown that leaf $\delta^{13}C$ was negatively correlated with a simple quantification of

environmental moistness, i.e. mean annual precipitation (MAP). However, exceptions of both positive correlations (e.g. Guo and Xie, 2006) and insignificant correlations (e.g. Turner et al., 2008) in arid or semiarid zones were reported. This effect is resulting from water stress physically influencing stomatal conductance and thus leaf $\delta^{13}C$, but precipitation is only one element in the water stress equation. This is probably why in some situations MAP does not directly correlate with leaf $\delta^{13}C$.

Recently it has been reported that a combination of soil moisture and potential evaporation, representing both water supply and demand effects, provides a better representation of water stress on plant transpiration than soil moisture only (Yang et al., 2013; Liu et al., 2017). The aridity index (AI), linking moisture supply and atmospheric demand for evaporation, is very likely a good representation of water stress. Therefore, we hypothesize that the leaf $\delta^{13}C$ value is correlated with the AI both in time and space. AI has been defined as PET/P (e.g., Budyko, 1974; Donohue et al., 2007; Gerrits, et al., 2009) and it can be easily calculated across different temporal and spatial scales.

In complex terrain, distribution of solar radiation often dominates among the local meteorological variables in determining plant water stress associated evaporative demand (Gutiérrez-Jurado, et al., 2006; Gutiérrez-Jurado, et al., 2013). Ridges, slopes, and depressions in complex terrain lead to a variety of different soil moisture conditions. Thus, complex terrain provides an excellent environment to

efficiently examine the lumped water stress on leaf $\delta^{13}C$.

In this study, we performed experiments in a native vegetation catchment with two opposite hillslopes, the north-facing slope (NFS, sunnier in the Southern Hemisphere) and the south-facing slope (SFS, more shady) in South Australia to examine the correlation between aridity index and leaf $\delta^{13}C$. The two opposite hillslopes of a V-shaped valley provided a broad range of hydro-climatic conditions to examine the influence of environmental factors on the leaf $\delta^{13}C$ value of individual trees. Leaves from three C_3 tree species, *Eucalyptus* (*E.*) *leucoxylon*, *E. paniculata* and *Acacia* (*A.*) *pycnantha* were sampled monthly over one year. In addition, we also collected leaf samples from *E. viminalis cygnetensis* twice along the study transect, at the end of the dry and the wet seasons. The specific objectives of this study were: 1) to understand the seasonality of leaf $\delta^{13}C$ for selected native tree species; 2) to understand spatial variation of leaf $\delta^{13}C$ due to different slope positions in the landscape; and 3) to evaluate the correlation between leaf $\delta^{13}C$ and the AI (PET/P) both in time and space.

2. Study site and materials

2.1. Study site

The study site is located at Mount Wilson (138.64˚ E, 35.21˚ S, 370 m a.s.l.) in the Mount Lofty Ranges of South Australia (Fig. 1). This study site is characterized

by a Mediterranean climate, being cold and humid in winter and hot and dry in summer. Long-term average annual total precipitation (1982 - 2013) of 716 ± 110 mm is dominated by winter rain events (http://www.bom.gov.au). In order to capture spatial variation of micro-meteorological conditions, three weather stations were installed at the study site (Fig. 1), one on each hillslope and one in a nearby open area.

<Figure 1 here please>

In this native vegetation site, *E. leucoxylon* and *E. paniculata* are dominant on the NFS and *E. viminalis cygnetensis* on the SFS. A transect including five trees on each slope was selected to conduct the experiments in this study (Fig. 1). These ten trees growing on two opposite hillslopes covered a wide range of gradual change of environmental conditions such as solar irradiance and the depth to groundwater.

Soil textures of the NFS and the SFS were determined using a sedimentation method based on the Stoke's Law. Five soil profiles (with varying thickness from 15 cm to 120 cm) were examined on each hillslope. Soil samples from each core were homogenised in 20 cm intervals, and percentages of three major grain-size fractions (clay, silt and sand) were calculated. In general, the ground surface on the NFS is rockier than on the SFS. The particle size factions for the upper 80 cm of soil are similar on both hillslopes (clay 15.6%, silt 33.9%, sand 51.5%; paired sample test, p-value = 0.66) while in the 80 - 120 cm depth interval, slightly more clay on the NFS (clay 16.7%, sand 52.0%) and more sand on the SFS (clay 11%, sand 58.2%) has been

observed.

2.2. Field sampling and sample storage

All trees selected for this study were about 13 m in height to avoid the uncertainty in data interpretation resulting from the tree height and the age effect (e.g. McDowell et al., 2011). From 31 August 2012 to 2 September 2013, 16 batches for 7 trees with 1 to 4 directions (211 samples), and 2 batches for other 3 trees with 1 to 4 directions (6 samples) of leaf samples were collected (in total 217 samples). Time interval between subsequent batches collection was about 20 days (Table 1). Leaf samples were collected from four sides (east, south, west, and north) of similar heights on each tree, except where a tree did not have a developed canopy in all desired directions. For each sampling batch, a total of 10 to 20 mature leaves were sampled and pooled together from each tree canopy section in a certain direction. Leaf samples were sealed in zip-lock bags and stored in a cold and dark ice-chest box. In the lab, the samples were dried at 70°C in an oven until a constant weight. Dry leaf samples were then grounded into powder and stored in sealed polyethylene jars.

<Table 1 here please>

All collected leaves were functionally mature. Carbon in the leaves has been accumulated over the leaf lifetime from initial development until the time of sampling. *E. leucoxylon*, *E. paniculata* and *E. viminalis cygnetensis* are species with broad

leaves that can be formed in pairs opposite one another for the whole life of the tree (https://www.anbg.gov.au). From our field observations, the new leaves of these three species were mainly formed in the wet season (June to October) and the leaves reached maturity in about two weeks. The first sample collection was on 31 August 2012, which was almost the end of the wet season. Our sample collection ended on 2 September 2013 and covered a whole growing season, providing representative samples for both wet and dry seasons and a whole year.

2.3. Stable carbon isotope analysis

The grounded leaf samples were analysed in the West Australian Biogeochemistry Centre at the School of Biological Sciences, The University of Western Australia, for $\delta^{13}C$, using a continuous flow system consisting of a Delta V Plus mass spectrometer connected with a Thermo Flush 1112 Elemental Analyser via Conflo IV (Thermo-Finnigan/Germany). The measured δ-values were normalised to VPDB (*Vienna Pee Dee Belemnitella americana*) isotope reference scale using the multi-point normalization technique and four international reference materials NBS19, L-SVEC, NBS22 and USGS24 (Skrzypek et al., 2010) and $\delta^{13}C$ was expressed in ‰ (Skrzypek, 2013). The external combined analytical uncertainty (one standard deviation) was 0.10‰.

3. Methods

3.1. Calculation of AI in time

In order to quantify the relationship between leaf $\delta^{13}C$ and plant water stress, daily PET (mm day^{-1}) was calculated using the Priestly-Taylor method (Priestly and Taylor, 1972) as shown in equation (1):

$$PET = \alpha \frac{\Delta}{\Delta + \gamma} \frac{R_n}{\lambda} \times \frac{10^3}{\rho} \qquad (1)$$

where α is the Priestly-Taylor coefficient assumed to be 1.26; Δ (kPa ˚C^{-1}) is the slope of the saturation vapour pressure-temperature relationship; γ (kPa ˚C^{-1}) is the psychrometric constant; R_n (MJ m^{-2} day^{-1}) is the net radiation above the surface observed by the weather station on the slope; λ is latent heat of vaporization, 2.45 MJ kg^{-1}; and ρ is water density, 1.0×10^3 kg m^{-3}. As the leaf $\delta^{13}C$ value is a time-accumulated signal reflecting the conditions of leaf growth over time, correspondingly AI for each sampling batch is calculated using equation (2):

$$AI = \sum_{t_0}^{t_i} PET \Big/ \sum_{t_0}^{t_i} P \qquad (2)$$

where t_0 is the beginning of the accumulation, and t_i refers to the date when the leaves were sampled, t_0 is varied in the analysis to find the most appropriate time point when the best correlation between AI and leaf $\delta^{13}C$ is found.

The daily P (mm/day) and PET (mm/day) are accumulated in such way because the exact start of the accumulating period of the leaf biomass (the start date of each

leaf growth) is unknown. Therefore, three different linear regression models for time series data of leaf $\delta^{13}C$ and AI have been tested. Firstly, we used the period between two consecutive sample batches as the accumulation time for the latter sampling batch ($t_0 = t_{i-1}$). On average we had around a 23-day sampling interval and we set a one-month period prior the first sampling batch. The first batch was collected on 31 August 2012 and the starting point for PET calculations was 1 August 2012 (the first t_0, when $i = 1$). Secondly, we used a two-month (61 days) period prior to the sampling date for each sampling batch. In other words, we assumed that carbon accumulating time period was 61 days until sample collection ($t_i - t_0 = 61$) and each sample reflects a running average condition over a 61-day window. The first t_0 was set as 2 July 2012, which was 61 days prior to the 31 August 2012. Thirdly, we applied the accumulation method with a constant t_0 of 1 August 2012 and t_i as the date of each sampling.

3.2. Calculation of AI in space

In order to quantify the relationship between leaf $\delta^{13}C$ and plant water stress level spatially, daily PET (mm day^{-1}) was calculated using equation (1) for each tree. As there was one weather station only on each hillslope, the net radiation used for PET calculation was calculated from the observed net radiation at a local weather station, and the ratio of global radiation at the tree geographic positions and that at the weather station. The global radiation was a sum of direct and diffuse radiation for different locations of the studied ten trees. It was calculated based on the

hemispherical viewshed algorithm (Rich et al., 1994; Fu and Rich, 2002) and a high resolution (1 m × 1 m) Digital Elevation Model (DEM) of the study area. The high resolution DEM was obtained by the airborne light detection and ranging technique (LiDAR). Then equation (2) was used for the calculation of spatial AI for each tree location, based on the accumulation method described previously.

3.3. Statistical analysis of the relationship between leaf $\delta^{13}C$ and AI

In order to evaluate the correlation between leaf $\delta^{13}C$ and environmental factors, linear regression was applied in time and space, respectively. Analysis of variance (ANOVA) table including significance level (p-value) was also obtained for each regression. Both a Student's *t* test and *F*-test were performed in the regression statistics, and the paired-sample *t* test for comparison of the cases between the two hillslopes.

4. Results

4.1. Seasonal variations of leaf $\delta^{13}C$

All mean $\delta^{13}C$ values of leaves from each tree were consistently more negative for the wet season than that for the dry season, although the difference was less than 1.1‰. The mean $\delta^{13}C$ value of leaves collected from each tree (10 in total) near the end of the dry season (5 March 2013) and at the end of the wet season (2 September

2013) along the sampling transect are shown on Fig. 2, panels A and B. Each point represents an average $\delta^{13}C$ value of samples collected from four different parts of the canopy, each part comprising 10 - 20 mature leaves collected from a branch facing one of the four directions, and error bars reflect standard deviations amongst samples from different directions. All leaf $\delta^{13}C$ values of 10 trees after the wet season were consistently lower than that after the dry season (p-value < 0.01), except tree S4 where no significant difference was observed (p-value > 0.98). The difference in leaf $\delta^{13}C$ between the two batches for each tree on average was 1.2 ± 0.4‰, which suggests significant seasonal variations.

<Figure 2 here please>

The leaf $\delta^{13}C$ values, across all locations and trees over 12 months, ranged from -32.6‰ to -28.9‰ (Table 2). The difference between the maximum and minimum $\delta^{13}C$ of leaves for each tree spanned from 1.2‰ to 2.7‰. Amongst all the trees, tree S5, located at the lowest and possibly wettest position in the landscape on the SFS (Fig. 1). It had the most negative maximum (-31.4‰) and minimum (-32.6‰) $\delta^{13}C$ of leaves in the whole sampling period and the smallest standard deviation (0.3‰) across the wet and the dry seasons.

<Table 2 here please>

We further examined temporal variation of leaf $\delta^{13}C$ for trees N1, N2, N4 and N5 on the NFS and trees S2, S4 and S5 on the SFS. (Fig. 3). Generally, leaf $\delta^{13}C$

progressively increased during the dry season and decreased during the wet season for both hillslopes. This pattern was clearly seen on the NFS while it was weaker on the SFS. The timing of the changes of these two trends was also quite consistent among the trees except tree S4, e.g. the regression between tree S2 and tree S5 has an adjusted $R^2 = 0.27$ with a p-value of 0.03.

<Figure 3 here please>

4.2. Spatial variations of leaf $\delta^{13}C$

Trees on the NFS had less negative leaf $\delta^{13}C$ values than trees on the SFS and the relative difference can be as large as 3.4‰ neglecting the difference in relative slope location (Fig. 3, and Table 2). Moreover, leaf $\delta^{13}C$ on the NFS started decreasing later than that on the SFS in the wet season. This is in agreement with the expected pattern, as the trees on the more shady SFS were subjected to a shorter water stress period due to lower solar radiation, lower surface temperature and consequently lower evaporative losses, and likely better soil moisture conditions than the NFS.

Tree N4 on the NFS and tree S4 on the SFS were both *A. pycnantha* and ~ 100 m apart from one another (Fig. 1) at a similar elevation. However, they had $\delta^{13}C$ difference of 1.7 ± 1.1‰ (p-value < 0.01), which suggested that tree N4 on the NFS was much more water-stressed than tree S4 on the SFS. In contrast, leaf $\delta^{13}C$ for tree S4 (*A. pycnantha*) was very similar to tree S5 (*E. leucoxylon*) in spite of the fact that

they belonged to two different genera. These two trees were located in the lowest section of the SFS slope at the bottom of the valley and likely experienced the lowest and shortest water stress.

On the other hand, trees located at the ends of expected aridity gradient on the SFS, tree S2 (*E. paniculata*) at the top part of the hillslope, and tree S4 (*E. leucoxylon*) at the bottom of the valley, had almost the same seasonal variation pattern in $\delta^{13}C$, despite very different values (2.1 ± 0.3‰) (Fig. 3). A few other examples confirmed that different species on the same hillslope, e.g. tree N1 and tree N4 on the NFS or tree S4 and tree S5 on the SFS, showed similar values and seasonal variations of leaf $\delta^{13}C$ through the monitoring year (Fig. 3 and Table 2).

4.3. Seasonal leaf $\delta^{13}C$ and AI

The leaf $\delta^{13}C$ is a transient signal that changes over time as new organic matter is produced under changing environmental conditions and added to the bulk leaf tissue produced before. Therefore, it always reflects a weighted mean, proportional to the pace of the leaf growth. In order to link $\delta^{13}C$ with seasonal weather conditions it would be important to know the weighted mean age of leaf carbon. We tested three different models since we do not know the exact age of carbon built into leaf tissues, assuming different carbon accumulation periods (see section 3.1.). The highest correlation and statistical significance were obtained for the model with constant t_0 set

on 1 August 2012, one month before first sampling (see the Appendix A and B, results from other two models). This model is also the closest one of the three that aligns with our expected understanding of the accumulated leaf $\delta^{13}C$ (section 2.2.).

The correlations between leaf $\delta^{13}C$ and AI were reasonably clear despite variability among individual trees (R^2 = 0.18 - 0.44 and p-value 0.00 - 0.06 for all trees on the NFS, Table 3). In contrast to the trees on the NFS, the trees on the SFS did not have statistically significant correlations between calculated AI and measured leaf $\delta^{13}C$ (R^2 = -0.07 - 0.13, p-value 0.10 - 0.73, Table 3).

<Table 3 here please>

4.4. Relationship of leaf $\delta^{13}C$ and AI in space

The relationship between leaf $\delta^{13}C$ and AI in space was examined using linear regression models for two selected sampling campaigns at the end of the dry and wet seasons, respectively (Table 4). The correlation was significant for the data sampled at the end of the dry season (5 March 2013, p-value 0.05) while insignificant for sampling at the end of the wet season (2 September 2013, p-value 0.13). Noticeably, the calculated change of 0.84‰ at the end of the dry season per AI unit variation across space was higher than a change of 0.21 ± 0.06‰ per AI unit variation in time on the NFS (Table 3).

<Table 4 here please>

The spatial relationship between leaf $\delta^{13}C$ and AI was re-examined using linear regression models for *E.* genus only (Table 4), resulting in a change of 0.74‰ per AI unit at the end of the dry season. This level of apparent dependency on AI was lower by 0.1‰ compared to that calculated for mixed *E.* and *A.* trees, and the correlation was statistically stronger and more significant (R^2 = 0.55 and p-value 0.04, instead of 0.35 and 0.05, respectively). The correlation was still insignificant at the end of the wet season.

5. Discussion

5.1. Local leaf $\delta^{13}C$ and its biochemical basis

The mean $\delta^{13}C$ value of all collected leaves in this study was -30.4 ± 1.1‰ (one standard deviation). As a comparison, the mean leaf $\delta^{13}C$ value of C_3 species growing in a MAP environment of 700 - 750 mm/year, similar to this study (716 mm/year), is calculated to be -26.4 ± 1.4‰, according to the global data compiled from the previous studies (Diefendorf et al., 2010; Cernusak et al., 2011; Miller at al., 2001; Schulze et al., 1998; Schulze et al., 2006; Sterwart et al., 1995; Turner et al., 2008). The more negative value found in this study may be related to the Mediterranean type climate in the study area where the maximum carboxylation occurs in spring when the water stress is low. It may also indicate that local baselines, which are composed of the upper and lower boundaries of the leaf $\delta^{13}C$ values in C_3 species, are closely

related to the local hydro-climate conditions (Farquhar and Sharkey, 1982; Ogaya and Peñuelas, 2008) and the local isotope signature of assimilated atmospheric CO_2. For a study that explores the climatic implication of leaf $\delta^{13}C$, local conditions such as slope orientation and possible seasonal leaf $\delta^{13}C$ variations need to be considered in addition to precipitation.

The general spatial trend is that trees on the SFS have more negative leaf $\delta^{13}C$ values than trees on the NFS, and trees at lower elevation have more negative leaf $\delta^{13}C$ values than trees at higher elevation (Table 2). Factors, other than precipitation, determining water availability arising from topography, such as soil moisture storage and solar irradiance need to be considered (Cernusak et al., 2005; Farquhar and Sharkey, 1982; Farquhar et al., 1989). Five soil profiles examined along each hillslope (Fig. 1) are not significant different in soil textures and soil depths, therefore differences in soil cannot be used to explain the general spatial trend. Usually the top part of a slope receives more solar irradiance, and the bottom part receives more water due to a larger flow accumulation. Both mechanisms lead to a typical spatial difference in soil moisture: dryer in the upper slope and wetter in the lower slope. This explains the observed systemic variations in leaf $\delta^{13}C$ along a slope. An equator-facing slope (e.g., the NFS in this study) receives more solar irradiance, and thus a larger deficit in soil moisture in the dry season (Yetemen et al., 2015) compared with polar-facing slope (e.g., the SFS), explaining the difference in leaf $\delta^{13}C$ between the two opposite hillslopes.

The stable carbon isotope fractionation in C_3 plants occurs during a two-step CO_2 uptake process. First, CO_2 diffuses through the stomata to the site of carboxylation, and second, intercellular CO_2 is taken up irreversibly by the carboxylase. The initial fractionation step is regulated by stomatal conductance which is highly correlated with water availability. If a plant is exposed to strong water stress, the stomata are nearly closed and the carboxylation process takes up virtually all intercellular CO_2 available, limiting initial fractionation. In consequence of the extreme low stomatal conductance, the $\delta^{13}C$ of the initial intercellular CO_2 used during carboxylation will approach -8‰ (O'Leary, 1981; Hersterberg and Siegenthaler, 1991). If the stomata are fully open and the conductance is high, the leaf intercellular CO_2 will be in equilibrium with the atmosphere. Initial CO_2 entering carboxylase will be fractionated, and CO_2 with lighter isotope ^{12}C will be assimilated preferentially over the heavier isotope ^{13}C (Roeske and O'Leary, 1984). In reality, the leaf $\delta^{13}C$ has intermediate values between these two extremes. This relationship can be qualitatively expressed as,

$$\delta^{13}C_{leaf} = [-4.4 + (-29 + 4.4) \times p_i/p_a] + \delta^{13}C_{atmospheric} \qquad (3)$$

where p_i is the internal gas-phase pressure of CO_2, and p_a is the ambient CO_2 pressure (Farquhar et al., 1989). More complex and accurate formulation has been reported, but the simplified one, equation (3), is sufficient for many applications (Cernusak et al., 2013), such as for this study.

Higher water availability for transpiration and photosynthesis is expected to result in a generally more negative leaf $\delta^{13}C$ as higher stomata conductivity results in an increased p_i and a larger isotope discrimination between atmospheric and cellular CO_2. Lower solar irradiance will also cause a reduction in leaf $\delta^{13}C$, as intercellular CO_2 pressure (p_i) will increase at lower light levels (Farquhar et al., 1989; Pearcy, 1988). Furthermore, it is also possible that the atmospheric CO_2 at the bottom of a valley has a lower $\delta^{13}C$ value than at the top of hillslopes due to higher contribution of CO_2 from soil respiration in a less ventilated position in the landscape (e.g., Fassbinder et al., 2012).

5.2. Leaf $\delta^{13}C$ can be a good proxy for temporal variation of water stress

Significant correlations between leaf $\delta^{13}C$ and AI on the NFS (Table 3) indicate that leaf $\delta^{13}C$ can be a good proxy for temporal variation of water stress (Ehleringer et al., 1992; Gao et al., 2006). On average, a decrease of one AI unit (wetter) can cause ~ 0.21 ± 0.06‰ decrease in leaf $\delta^{13}C$ (more negative). However, it will also depend on the ratio that leave weights versus the organic matter weights added during each period of growth between sampling campaigns (Farquhar and Sharkey, 1982; Cernusak et al., 2013). Therefore, the uncertainty of an estimation of accumulated AI can be large, and that the timing of rainy season should be considered in sampling procedures.

Correlations between leaf $\delta^{13}C$ and AI on the SFS were insignificant (Table 3). AI on the SFS was consistently lower (wetter) than that on the NFS throughout the whole monitoring year and this difference can be as large as 2.3 AI units. Therefore, the water stress on the SFS was generally lower in comparison to the NFS, particularly for tree S4. Also the water availability along the SFS may not be determined exclusively by AI but likely other environmental parameters (Farquhar and Sharkey, 1982; Cernusak et al., 2009), e.g., depth of soil might have played a more important role resulting in an inconsistent $\delta^{13}C$ signal along the AI gradient. Despite large differences between individual trees, samples collected on the SFS generally had more negative $\delta^{13}C$ values than those from the NFS, this is consistent with the expected pattern of lower leaf $\delta^{13}C$ in less arid locations (Table 3).

While the correlations between AI and leaf $\delta^{13}C$ were significant on the NFS, the correlations between precipitation only and leaf $\delta^{13}C$ were insignificant on either hillslope (p-value 0.07 - 0.85, Table 3). These results suggest that it is more appropriate to use AI rather than precipitation to represent seasonal variation of plant water stress, which is reflected in leaf $\delta^{13}C$. Small differences between species were not visible on the temporal trend plots (Fig. 2), however, they were large enough to display significant differences when linear regression models were used (Table 3).

5.3. Leaf $\delta^{13}C$ can be used as a proxy for plant water stress across landscapes

Without considering tree genera, significant correlation between leaf $\delta^{13}C$ and AI following the dry season is shown in Table 4. This suggests that leaf $\delta^{13}C$ can be used as a valuable proxy for plant water stress at a local scale as well as other studies across the landscape (e.g. Stewart et al., 1995; Guo and Xie, 2006). However, the correlation was insignificant at the end of the wet season suggesting that during the wet season trees were not water stressed significantly enough to result in differences in $\delta^{13}C$, or that factors other than AI could influence $\delta^{13}C$, such as tree species with different water use efficiency (Farquhar et al., 1989; Tanaka-Oda et al., 2010).

When tree genus is considered, there is a slightly more significant correlation between leaf $\delta^{13}C$ and AI following the dry season (Table 4) for *E.* trees. It indicates that spatial variations of leaf $\delta^{13}C$ may be related to tree species. The results that a large spatial variation of leaf $\delta^{13}C$ during the dry season only suggests, the spatial difference in hydro-climatic conditions is larger along the observation transect during the dry season than that in the wet season.

To examine if a similar relationship exists on the large scale, the correlation between leaf $\delta^{13}C$ and AI was compared with that between leaf $\delta^{13}C$ and precipitation using the compiled data from the previous large-scale studies (Diefendorf et al., 2010; Cernusak et al., 2011; Miller at al., 2001; Schulze et al., 1998; Schulze et al., 2006; Sterwart et al., 1995; Turner et al., 2008) (Fig. 4). For the data with MAP less than 1000 mm/year, under which vegetation is very likely under water stress, AI has a

better correlation with leaf $\delta^{13}C$ than precipitation. On the other hand, precipitation is better correlated with leaf $\delta^{13}C$ than AI for the data with MAP in a range of 1000 - 2000 mm/year, but in this range of precipitation, plants are unlikely under water stress (Kohn, 2010). Thus, it appears that AI represents plant water stress better than precipitation, and there is a large-scale generalized relationship between leaf $\delta^{13}C$ and AI.

<Figure 4 here please>

In this study, we applied the Priestly-Taylor equation to calculate AI in space (section 3.2), only solar irradiance was interpolated to each tree location due to a lack of meteorological data for every sampled tree. However, solar irradiance can also cause a change in leaf $\delta^{13}C$ (Ehleringer et al., 1986). Simultaneously, solar irradiance determines PET and thus AI, which may result in a change in leaf $\delta^{13}C$ as well. Therefore, it is difficult to distinguish the two mechanisms in the field (Farquhar et al., 1989).

5.4. Implications for using plant carbon isotopic data in climate and ecohydrological studies

The hydro-climatic dependency (the coefficient in the regression function (Table 3 and 4)) revealed from the spatial data at the end of the dry season is three times larger than that from the seasonal data on the NFS. This finding supports the use

of carbon isotope data derived from plant tissues to detect the change of mean climatic condition. Such detection is likely to work not only at a local scale according to this study but also in broad climatic zones, e.g. precipitation less than 1000 mm/year (synthesized studies in Fig. 4).

The magnitude of seasonal variation in leaf $\delta^{13}C$ is similar to the spatial variation of leaf $\delta^{13}C$ along 2 - 3 AI units of hydro-climatic gradient. This finding stresses the importance in obtaining temporally representative data to construct carbon isotope and climate relationships. The clear seasonal variations in leaf carbon $\delta^{13}C$ also suggest that the matured leaves of the studied species can reflect the accumulated seasonal hydro-climatic signals. Environmental conditions appear to be powerful drivers of the leaf $\delta^{13}C$ value outweighing to a large extent physiological differences among the studied species. This finding supports the practice of pooling leaves of different species together to derive the relationship between $\delta^{13}C$ and climate variables.

5.5. Strength and limitation of this study

This study was focused on both spatial and temporal variations of leaf $\delta^{13}C$. Selection of the study site along a steep topographic gradient characterized by a broad range of micro-environmental and hydrological conditions allowed successful observation of tree responses to water stress, recorded in the stable carbon isotope

compositions of leaves. We continuously collected 199 quasi-monthly leaf samples. Each quasi-monthly sample was a pool of 10 - 20 leaves (in one direction) collected from each of four different directions of each tree. Due to this high frequency and relatively long sampling duration, we selected a relatively small number of trees (ten trees). For each species, only two to four individual trees were sampled. The small number of sampled trees inevitably introduces some uncertainty. Nevertheless, the result indicates that the effect from the topographically induced hydro-climatic condition outweighs the difference among tree species. This finding supports the reliability of the sampling design employed in this study.

It should also be noticed that by using the Priestly-Taylor (1972) PET formulation, variation in PET due to variation in wind-speed is not incorporated into the PET (Donohue et al., 2010; McKenney and Rosenberg, 1993; McVicar et al., 2012). However, this has little effects on the comparison between leaf $\delta^{13}C$ and AI, due to the highly similar daily-mean wind speed (m/sec) between the NFS and the SFS ($W_{NFS} = 0.98W_{SFS} + 0.08$, $R^2 = 0.98$, p-value 0.00), and high correlations of paired-samples 0.99 with p-value 0.00.

6. Conclusions

Significant seasonal variations, calculated as difference between the maximum and minimum values for each tree, were observed in leaf $\delta^{13}C$ for the studied trees.

Also the difference in leaf $\delta^{13}C$ observed between two opposite hillslopes was statistically significant (p-value 0.02) with the mean difference of 1.4 ± 0.5‰. Significant correlation between leaf $\delta^{13}C$ and AI was observed across time in locations exposed to the higher water stress on the north-facing slope, and across locations at the end of the dry season. In contrast, correlations for the relatively wetter south-facing slope and downslope locations, and for the time at the end of the wet season, were not statistically significant.

These results suggest that both temporal and spatial variations in aridity are important drivers of leaf $\delta^{13}C$ with more arid conditions causing water stress resulting in relatively less negative $\delta^{13}C$ in leaves, and that leaf $\delta^{13}C$ can be a good indicator for both seasonal and spatial variations of plant water stress.

Acknowledgements

This study was funded by National Centre for Groundwater Research and Training, Australia. The first author was supported by the China Scholarship Council, and by the Fundamental Research Funds for the Central Universities [lzujbky-2016-158]. Grzegorz Skrzypek is supported by a Future Fellowship from the Australian Research Council [FT110100352]. The authors thank Hailong Wang, Robert Andrew, Hugo Gutierrez-Jurado, Yuting Yang, Zijuan Deng and Yunquan Wang for their assistance in the field work, and John Hutson for providing advice on

soil texture analysis in the lab. Langdon Badger kindly provided the permission and necessary support to access the field site. Ashleigh Pitman from Willunga Environment Centre and Paul Green from Flinders University provided the identification of the tree species.

The authors appreciate the constructive comments from the editors, Stephen P. Good and one anonymous reviewer.

References

Budyko, M.I., 1974. Climate and life. *Int. Geophys. Ser*. 18. Academic press New York, New York.

Cernusak, L. A., Farquhar, G. D., Pate, J. S., 2005. Environmental and physiological controls over oxygen and carbon isotope composition of Tasmanian blue gum, Eucalyptus globulus. *Tree Physiol.* 25, 129 - 146.

Cernusak, L.A., Hutley, L.B., Beringer, J., Holtum, J.A.M., Turner, B.L., 2011. Photosynthetic physiology of eucalytpts along a sub-continental rainfall gradient in northern Australia. *Agric. For. Meteorol.* 151, 1462 - 1470.

Cernusak, L. A., Tcherkez, G., Keitel, C., Cornwell, W. K., Santiago, L. S., Knohl, A., Barbour. M.M., Williams, D.G., Reich, P.B., Ellsworth, D.S., Dawson, T.D., Griffiths, H.G., Farquhar, G.D., Wright, I.J., 2009. Why are non-photosynthetic tissues generally ^{13}C enriched compared with leaves in C_3 plants? Review and synthesis of current hypotheses. *Funct. Plant Biol.* 36(3), 199 - 213.

Cernusak, L.A., Ubierna, N., Winter, K., Holtum, J.A.M., Marshall, J.D., Farquhar, G.D., 2013. Environmental and physiological determinants of carbon isotope discrimination in terriestrial plants. *New Phytol.* 200, 950 - 965.

Dawson, T. E., Ehleringer, J. R., 1991. Streamside trees that do not use stream water. *Nature*. 350 (6316), 335 - 337.

Diefendorf, A.F., Mueller, K.E., Wing, S.L., Koch, P.L., Freeman, K.H., 2010. Global patterns in leaf ^{13}C discrimination and implications for studies of past and future climate. *Proc. Natl. Acad. Sci.*107 (13), 5738 - 5743.

Donohue, R.J., McVicar, T.R., Roderick, M.L., 2010. Assessing the ability of potential evaporation formulations to capture the dynamics in evaporative demand within a changing climate. *J. Hydro.* 386(1-4), 186 - 197.

Donohue, R.J., Roderick, M.L., McVicar, T.R., 2007. On the importance of including vegetation dynamics in Budyko's hydrological model. *Hydrol. Earth Syst. Sci.* 11(2), 983-995.

Ehleringer, J.R., Field, C.B., Lin, Z.F., Kuo, C.Y., 1986. Leaf carbon isotope ratio and mineral composition in subtropical plants along an irradiance cline. *Oecologia.* 70, 520 - 26.

Ehleringer, J.R., Phillips, S.L., Comstock, J.P., 1992. Seasonal variation in the carbon isotopic composition of desert plants. *Funct. Ecol*. 6, 396 - 404.

Evans, J.R., von Caemmerer, S., 2013. Temperature response of carbon isotope discrimination and mesophyll conductance in tobacco. *Plant Cell Environ*. 36, 745 - 756.

Farquhar, G.D., Sharkey, T.D., 1982. Stomatal conductance and photosynthesis. *Annu. Rev. Aust. J. Plant Physiol.* 11, 539 - 552.

Farquhar, G.D., Ehleringer J.R., Hubick K.T., 1989. Carbon isotope discrimination and photosynthesis. *Annu. Rev. Plant Physiol. Plant Mol. Biol*. 40, 503 - 537.

Fassbinder, J.J., Griffis T.J., Baker J.M., 2012. Interannual, seasonal, and diel variability in the carbon isotope composition of respiration in a C_3/C_4 agricultural ecosystem. *Agric. For. Meteorol*. 153, 144 - 153.Fu, P., Rich, P.M., 2002. A Geometric Solar Radiation Model with Applications in Agriculture and Forestry. *Comput. Electron. Agric.* 37, 25 - 35.

Gao, T.P., Chen, T., Feng, H.Y., An. L. Z., Xu, S.J., Wang, X.L., 2006. Seasonal and annual variation of osmotic solute and stable carbon isotope composition in leaves of endangered desert evergreen shrub *Ammopiptanthus mongolicus*. *S. Afr. J. Bot*. 72, 570 - 578.

Gerrits, A.M.J., Savenije, H.H.G., Veling, E.J.M., Pfister, L., 2009. Analytical derivation of the Budyko curve based on rainfall characteristics and a simple evaporation model. *Water Resour. Res*. 45, W04403.

Good, S.P., Caylor, K.K., 2011. Climatogical determinants of woody cover in Africa. *Proc. Natl. Acad. Sci.* 108(12): 4902 - 4907.

Guo, G., Xie, G., 2006. The relationship between plant stable carbon isotope composition, precipitation and satellite data, Tibet Plateau, China. *Quat. Int.* 144(1), 68 - 71.

Gutiérrez-Jurado, H.A., Vivoni, E.R., Cikoski, C., Harrison, J.B.J., Bras, R.L.,

Istanbulluoglu, E., 2013. On the observed ecohydrologic dynamics of a semiarid basin with aspect-delimited ecosystems. *Water Resour. Res.* 49(12), 8263 - 8284.

Gutiérrez-Jurado, H.A., Vivoni, E.R., Harrison, J.B.J., Guan, H., 2006. Ecohydrology of root zone water fluxes and soil development in complex semiarid rangelands. *Hydrol. Process*. 20(15), 3289 - 3316.

Guy, R.D., Fogel, M.F., Berry, J.A., Hoering, T.C., 1987. Isotope fractionation during oxygen production and consumption by plants. *Prog. Photosynth. Res.* III, 597 - 600.

Hesterberg, R., Siegenthaler, U., 1991. Production and stable isotopic composition of CO_2 in a soil near Bern, Switzerland. *Tellus*. 43B, 197 - 205.

Jarvis, P.G., 1976. The interpretation of the variations in leaf water potential and stomatal conductance found in canopies in the field. *Philos. Trans. R. Soc. London B*. 273(927), 593 - 610.

Kohn, M.J., 2010. Carbon isotope compositions of terrestrial C_3 plants as indicators of (paleo)ecology and (paleo)climate. *Proc. Natl. Acad. Sci.* 107(46), 19691 - 19695.

Liu, B., Guan, H., Zhao, W., Yang, Y., Li, S., 2017. Groundwater facilitated water-use efficiency along a gradient of groundwater depth in arid northwestern China. *Agric. For. Meteorol*. 233, 235 - 241.

Liu, N., Guan, H., Luo, Z., Zhang, C., Wang H., Zhang, X., 2017. Examination of a coupled supply- and demand-induced stress function for root water uptake modelling. *Hydro. Res.* 48(1), 66 - 76.

Lloret, F., Peñuelas, J., Ogaya, R., 2003. Establishment of co-existing Mediterranean tree species under a varying soil moisture regime. *J. Veg. Sci.* 15(2), 237 - 244.

Lubczynski, M. W., 2009. The hydrogeological role of trees in water-limited environments. *Hydrogeo. J.* 17(1), 247 - 259(13).

McDowell, B.J., Dickman, L.T., Ryan, M.G., Whitehead, D., 2011. Relationships between tree height and carbon isotope discrimination. In: Meinzer F.C., Lachenbruch, B., Dawson, T.E., eds. *Size- and age-related changes in tree structure and function*. New York, NY, USA: Springer, 255 - 285.

McDowell, N., Pockman, W. T., Allen, C. D., Breshears, D. D., Cobb, N., Kolb, T., Plaut, J., Sperry, J., West A., Williams, D.G., Yepez, E.A., 2008. Mechanisms of plant survival and mortality during drought: why do some plants survive while others succumb to drought? *New Phytol.* 178(4), 719 - 739.

McKenney, M.S., Rosenberg, N.J., 1993. Sensitivity of some potential evapotranspiration estimation methods to climate change. *Agric. For. Meteorol*. 64(1-2), 81 - 110.

McVicar, T.R., Roderick, M.L., Donohue, R.J., Li, L.T., Van Niel, T.G., Thomas, A., Grieser, J., Jhajharia, D., Himri, Y., Mahowald, N.M., Mescherskaya, A.V., Kruger, A.C., Rehman, S., Dinpashoh, Y., 2012. Global review and synthesis of trends in observed terrestrial near-surface wind speeds: Implications for evaporation. *J. Hydrol.* 416-417, 182 - 205.

Miller, J.M., Williams, R.J., Farquhar, G.D., 2001. Carbon isotope discrimination by a consequence of *Eucalyptus* species along a subcontinental rainfall gradient in Australia. *Funct. Ecol*. 15, 222 - 232.

Nemani, R.R., Keeling, C.D., Hashimoto, H., Jolly, W.M., Piper, S.C., Tucker, C.J., Myneni, R.B., Running, S.W., 2003. Climate-driven increases in global terrestrial net primary production from 1982 to 1999. *Science*, 300(5625), 1560 - 1563.

Ogaya, R., Peñuelas, J., 2008. Changes in leaf $\delta^{13}C$ and $\delta^{15}N$ for three Mediterranean tree species in relation to soil water availability. *Acta Oecol.* 34(3): 331 - 338.

O'Leary M.H., 1981. Carbon isotope fractionation in plants. *Phytochemistry.* 20, 553 - 567.

Pearcy, R.W., 1988. Photosynthetic utilization of lightflecks by understory plants. *Aust. J. Plant Physiol.* 15, 223 - 238.

Priestley, C.H.B., Taylor, R.J., 1972. On the assessment of surface heat flux and evaporation using large-scale parameters. *Mon. Weather Rev.* 100 (2), 81 - 92.

Rich, P. M., R. Dubayah, W. A. Hetrick, Saving, S.C., 1994. Using Viewshed Models to Calculate Intercepted Solar Radiation: Applications in Ecology. American Society for Photogrammetry and Remote Sensing Technical Papers, 524 - 529.

Roeske, C.A., O'Leary, M.H., 1984. Carbon isotope effects on the enzyme catalyzed carboxylation of ribulaose bisphosphate. *Biochem*. 23, 6275 - 6284.

Sardans, J., Peñuelas, J., 2013. Plant-soil interactions in Mediterranean forest and shrublands: Impacts of climatic change. *Plant Soil*. 365(1/2), 1 - 33.

Schmidt, H.L., Winkler, F. J., Latzko, E., Wirth, E., 1978. ^{13}C-Kinetic isotope effects in photosynthetic carboxylation reactions and $\delta^{13}C$-values of plant material. *Isr. J. Chem*. 17, 223 - 224.

Schulze, E.-D., Turner, N.C., Nicolle, D., Schumacher, J., 2006. Leaf and wood carbon isotope ratios, specific leaf areas and wood growth of Eucalyptus species across a rainfall gradient in Australia. *Tree Physiol*. 26, 479 - 492.

Schulze, E.-D., Williams, R.J., Farquhar, G.D., Schulze, J.L., Miller, J.M., Walker, B.H., 1998. Carbon and nitrogen isotope discrimination and nitrogen nutrition of trees along a rainfall gradient in northern Australia. *Aust. J. Plant Physiol.* 25, 413 - 425.

Skrzypek, G., 2013. Normalization procedures and reference material selection in stable HCNOS isotope analyses-an overview. *Anal. Bioanal. Chem.* 405, 2815 - 2823.

Skrzypek, G., Kałużny, A., Wojtuń, B, Jędrysek, M.O., 2007. The carbon stable isotopic composition of mosses - the record of temperature variations. *Org. Geochem.* 38, 1770 - 1781.

Skrzypek, G., Sadler, R., Paul, D., 2010. Error propagation in normalization of stable isotope data: a Monte Carlo analysis. *Rapid Commun. Mass Spectrom.* 24, 2697 - 2705.

Skrzypek, G., Paul, D., Wojtuń, B., 2013. The altitudinal climatic effect on the stable isotope compositions of Agave and Opuntia in arid environments - a case study at the Big Bend National Park, Texas, USA. *J. Arid Environ.* 92, 102 - 112.

Smith B.N., Oliver J., Mc Millan, C.,1976. Influence of Carbon Source, Oxygen Concentration, Light Intensity, and Temperature on $^{13}C/^{12}C$ Ratios in Plant Tissues. *Bot. Gaz.* 137(2), 99 - 104.

Stewart, G.R., Turnbull, M.H., Schmidt, S., Erskine, P.D., 1995. ^{13}C Natural abundance in plant communities along a rainfall gradient: a biological integrator of water availability. *Aust. J. Plant Physiol.* 22, 51 - 55.

Tanaka-Odaa, A., Kenzob, T., Koretsunea, S., Sasakic, H., Fukudaa, K., 2010. Ontogenetic changes in water-use efficiency ($\delta^{13}C$) and leaf traits differ among tree species growing in a semiarid region of the Loess Plateau, China. *For. Ecol. Manag.* 259(5), 953 - 957.

Troughton, J.H., Card, K.A., 1975. Temperature effects on the carbon-isotope ratio of C_3, C_4 and crassulacean-acid-metabolism (CAM) plants. *Planta*, 123(2), 185 - 190.

Turner, N.C., Schulze, E.-D., Nicolle, D., Schumacher, J., Kuhlmann, I., 2008. Annual rainfall does not directly determine the carbon isotope ratio of leaves of *Eucalyptus* species. *Physiol. Plant*. 132, 440 - 445.

van Groenigen, J.W., van Kessel, C., 2002. Salinity-induced patterns of natural abundance carbon-13 and nitrogen-15 in plant and soil. *Soil Sci. Soc. Am. J.* 66, 489 - 498.

Vicente-Serrano, S.M., Gouveia, C., Camarero, J.J.J.; Beguería, S., Trigo R., López-Moreno, J.I., Azorín-Molina, C., Pasho, E., Lorenzo-Lacruz, J., Jesús Revuelto, J., Morán-Tejeda, E., Sanchez-Lorenzo, A., 2013, Response of vegetation to drought time-scales across global land biomes. *Proc. Natl. Acad. Sci. U.S.A.* 110(1), 52 - 57.

Wang, H., Guan, H., Deng, Z., Simmons, C.T., 2014, Optimization of canopy conductance models from concurrent measurements of sap flow and stem water potential on Drooping Sheoak in South Australia, *Water Resour. Res.* 50, 6154 - 6167.

Wang, H., Guan, H., Simmons, C.T., 2016. Modeling the environmental controls on tree water use at different temporal scales. *Agric. For. Meteorol.* 225, 24 - 35.

Yang, Y., Guan, H., Hutson, J.L., Wang, H., Ewenz, C., Shang, S., Simmons, C.T., 2013. Examination and parameterization of the root water uptake model from stem water potential and sap flow measurements. *Hydro. Process.* 27(20), 2857 - 2863.

Yetemen, O., Istanbulluoglu, E., Flores-Cervantes, J.H., Vivoni, E.R., Bras R.L., 2015. Ecohydrologic role of solar radiation on landscape evolution. *Water Resour. Res.* 51 (2), 1127 - 1157.

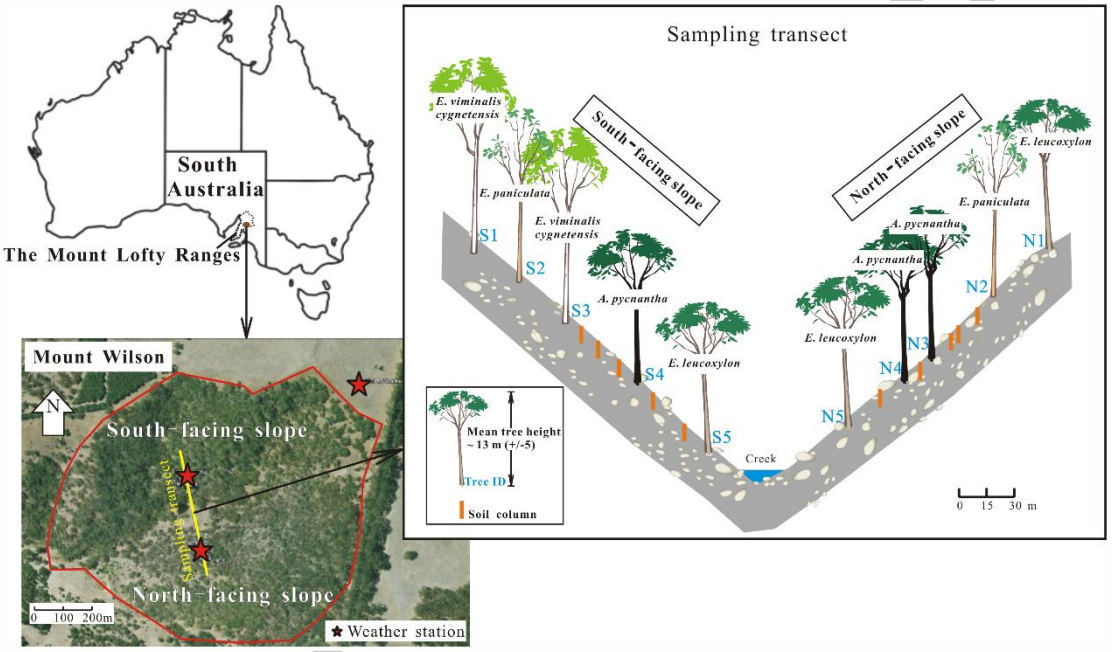

Figure 1. The conceptual diagram of the sampling design at the Mount Wilson study site (138.64˚ E, 35.21˚ S, 370 m a.s.l.) with locations of ten sampling trees on the two opposite hillslopes in South Australia.

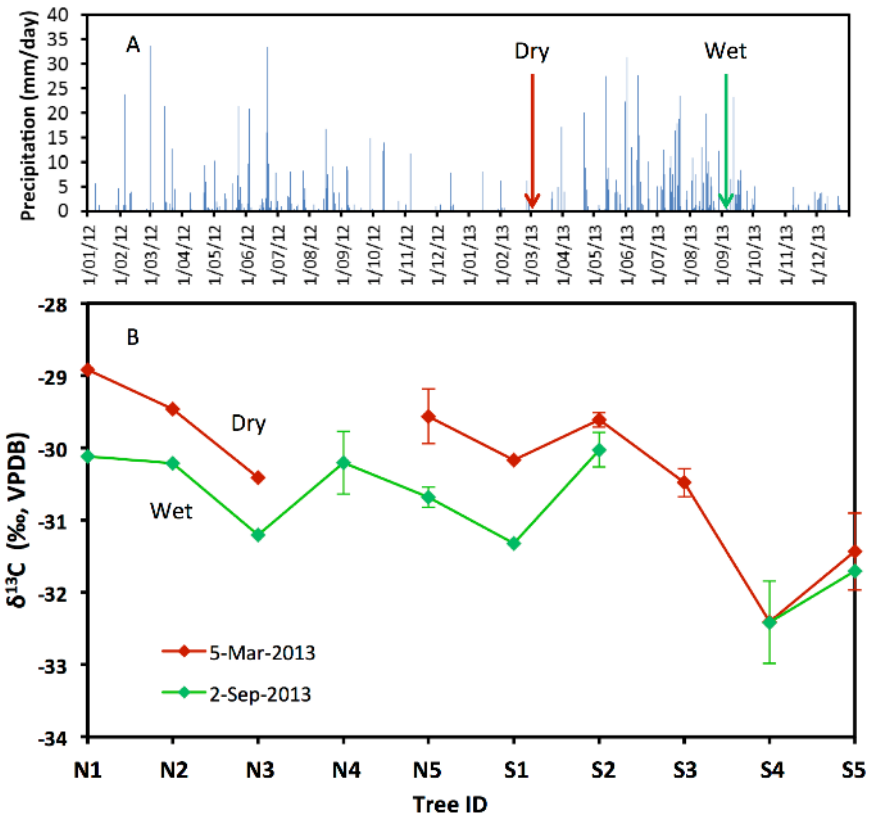

Figure 2. Daily precipitation between 1 January 2012 and 12 December 2013 at the Mount Wilson study site (A) and leaf $\delta^{13}C$ of the ten trees (B) sampled across the elevation gradient after the dry (5 March 2013) and wet (2 September 2013) seasons.

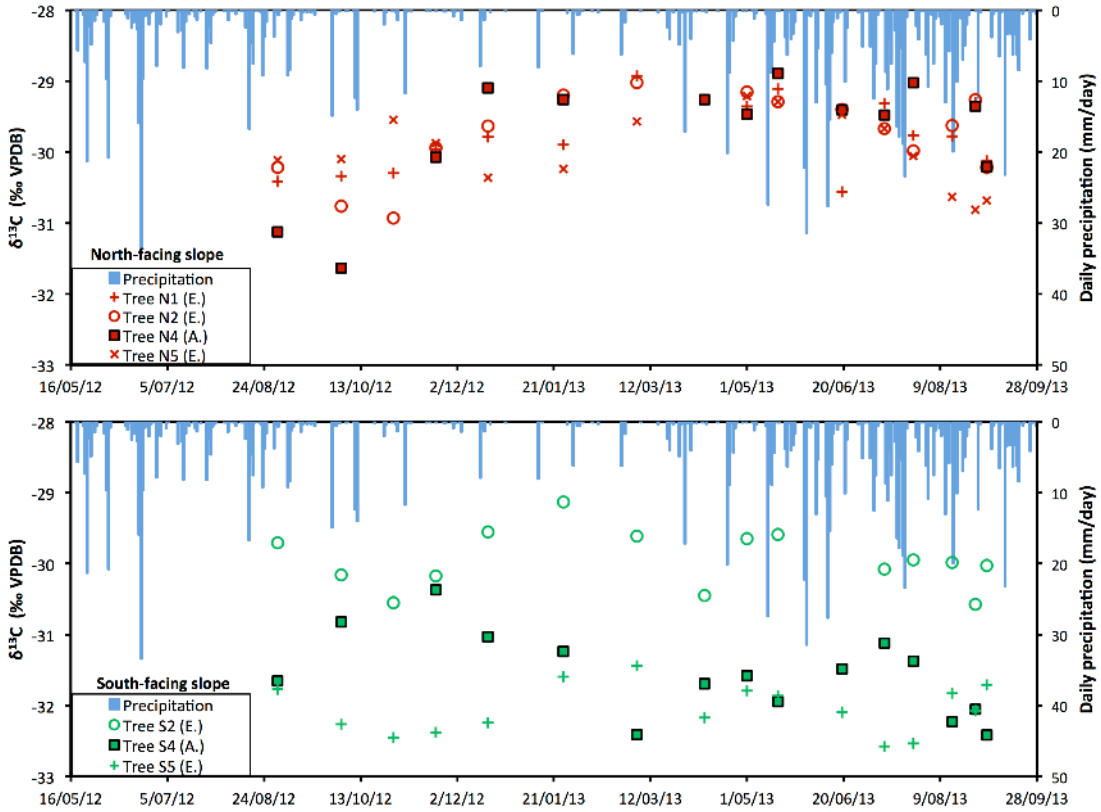

Figure 3. Time series data of leaf $\delta^{13}C$ of *Eucalyptus* (*E.*) *leucoxylon* (crosses), *Eucalyptus* (*E.*) *paniculata* (open circles) and *Acacia* (*A.*) *pycnantha* (close squares) on the two opposite hillslopes.

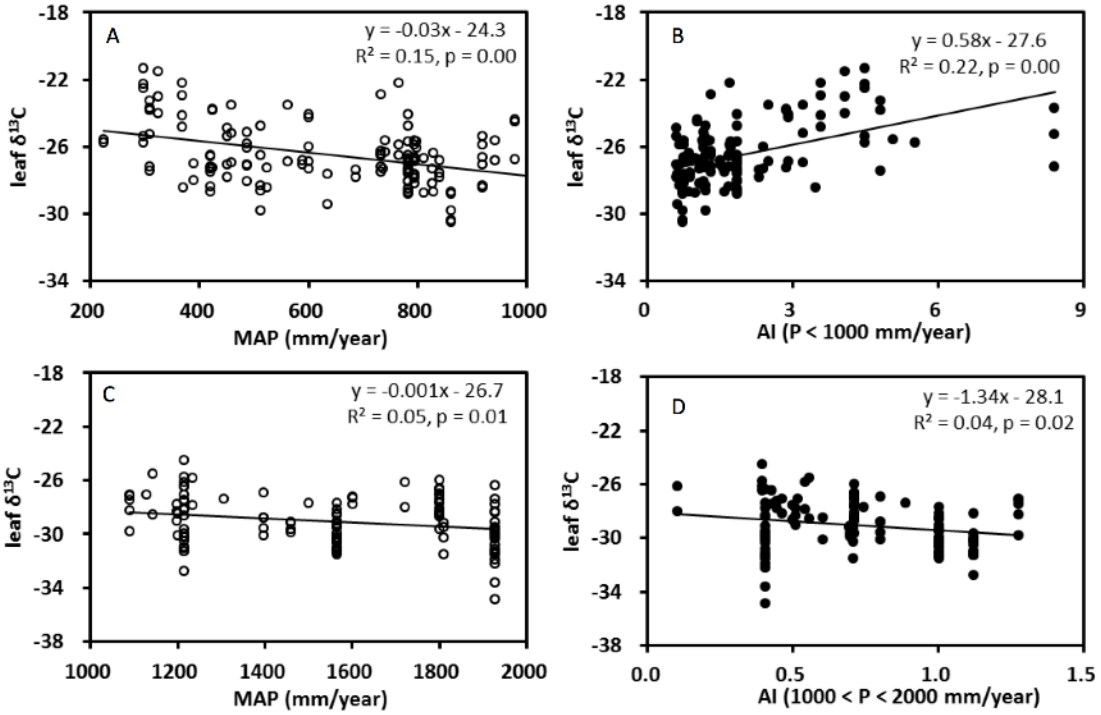

Figure 4. The leaf $\delta^{13}C$ values of various tree species for multiple locations from Europe, North America, Asia, Oceania and Southern Africa (summarized from Diefendorf et al., 2010; Cernusak et al., 2011; Miller et al., 2001; Schulze et al., 1998; 2006; Stewart et al., 1995; Turner et al., 2008). Correlations between leaf $\delta^{13}C$ and mean annual precipitation (MAP) are shown in the panel A (MAP < 1000 mm/year) and the panel C (1000 < MAP < 2000 mm/year), while correlations between leaf $\delta^{13}C$ and the aridity index (AI) are presented in the panel B (MAP < 1000 mm/year) and the panel D (1000 < MAP < 2000 mm/year).

Table 1. Details of sample collection at Mount Wilson site. Including sampling dates, numbers collected (N), accumulated potential evapotranspiration (PET), accumulated precipitation (P), and corresponding aridity index (AI, PET/P) on the north-facing slope (NFS) and the south-facing slope (SFS) start from 1 August 2012 and end to the sampling date.

Date	**N**	**PET (NFS, mm)**	**PET (SFS, mm)**	**P (mm)**	**AI (NFS)**	**AI (SFS)**
31-Aug-12	14	82.9	49.8	53.5	1.5	0.9
03-Oct-12	13	283.6	200.9	92.4	3.1	2.2
30-Oct-12	7	528.8	396.0	121.6	4.3	3.3
21-Nov-12	17	764.0	585.1	135.6	5.6	4.3
18-Dec-12	16	1051.2	815.8	148.9	7.1	5.5
26-Jan-13	17	1559.0	1229.9	157.4	9.9	7.8
05-Mar-13	14	1948.3	1541.2	173.7	11.2	8.9
09-Apr-13	6	2190.2	1726.4	207.8	10.5	8.3
01-May-13	16	2298.8	1805.1	242.7	9.5	7.4
17-May-13	16	2360.3	1847.7	292.2	8.1	6.3
19-Jun-13	13	2446.3	1898.8	447.9	5.5	4.2
11-Jul-13	17	2511.5	1939.8	496.4	5.1	3.9
26-Jul-13	15	2547.8	1960.6	613.2	4.2	3.2
15-Aug-13	9	2613.9	2004.4	668.8	3.9	3.0
27-Aug-13	11	2651.6	2028.6	722.8	3.7	2.8
02-Sep-13	16	2687.4	2055.4	735.5	3.7	2.8

Table 2. Leaf $\delta^{13}C$ (in ‰) from 31 August 2012 to 2 September 2013 for all the tree species at Mount Wilson.

Site	Tree ID	Tree species	$\delta^{13}C$(‰, VPDB) range	$\delta^{13}C$ (‰, VPDB) mean (±SD)	$\delta^{13}C$ (‰, VPDB) dry season* mean (±SD)	$\delta^{13}C$ (‰, VPDB) wet season* mean (±SD)	Annual global radiation ($\times 10^6$ Wh/m^2/year)
North-facing slope	N1	*E. leucoxylon*	-30.6 - -28.9	-29.8 (±0.5)	-29.5 (±0.5)	-29.9 (±0.4)	1.281
	N2	*E. paniculata*	-30.9 - -29.0	-29.7 (±0.6)	-29.3 (±0.3)	-30.1 (±0.6)	1.270
	N3	*A. pycnantha*	N/A	N/A	-30.4	-31.2	1.262
	N4	*A. pycnantha*	-31.6 - -28.9	-29.7 (±0.8)	-29.2 (±0.1)	-30.1 (±1.1)	1.260
	N5	*E. leucoxylon*	-30.8 - -29.2	-30.0 (±0.5)	-30.1 (±0.4)	-30.2 (±0.5)	1.282
South-facing slope	S1	*E. viminalis cygnetensis*	N/A	N/A	-30.2	-31.3	0.934
	S2	*E. paniculata*	-30.6 - -29.1	-29.9 (±0.4)	-29.4 (±0.3)	-30.1 (±0.3)	0.806
	S3	*E.viminalis cygnetensis*	N/A	N/A	-30.5	N/A	0.785
	S4	*A. pycnantha*	-32.4 - -30.4	-31.6 (±0.6)	-31.6 (±0.7)	-31.7 (±0.6)	0.809
	S5	*E. leucoxylon*	-32.6 - -31.4	-32.0 (±0.3)	-31.8 (±0.4)	-32.1 (±0.4)	0.775

*The dry season is from November to March and the wet season is from June to October.
N/A-not available, and tree N3, tree S1 and tree S3 were sampled twice only.

Table 3. Regression equations, R^2 and p-value are results from linear regression models for time series data of leaf $\delta^{13}C$ and aridity index (AI) for species of two genera: *Eucalyptus* and *Acacia* trees. The last column shows the p-value from the linear regression models for time series data of leaf $\delta^{13}C$ and precipitation (P, mm accumulated from 1 August 2012 to the sampling date). Regression equations are not shown when p-value > 0.05.

Site	**Tree ID***	**Regression equations**	**R^2 (adjusted)**	**p-value (AI)**	**p-value (P, mm)**
North-facing slope	N1	$\delta^{13}C = 0.16 \times (PET/P) - 30.4$	0.30	0.00	0.55
	N2	$\delta^{13}C = 0.20 \times (PET/P) - 30.5$	0.44	0.00	0.59
	N4	$\delta^{13}C = 0.27 \times (PET/P) - 30.8$	0.30	0.03	0.24
	N5		0.18	0.06	0.07
South-facing slope	S2		0.13	0.10	0.32
	S4		-0.07	0.73	0.07
	S5		0.10	0.13	0.85

Table 4. Linear regression results for spatial variations of leaf $\delta^{13}C$ and aridity index including the two genera, *Eucalyptus* (*E.*) and *Acacia* (*A.*) trees, and for the genus *E.* trees at Mount Wilson. Regression equations are not shown when p-value > 0.05.

Genus	**Date**	**Regression equations**	**R^2 (adjusted)**	**p-value**
E. and *A.* trees	2013-Mar-05	$\delta^{13}C = 0.84 \times (PET/P) - 35.8$	0.35	0.05
	2013-Sep-02		0.20	0.13
E. trees	2013-Mar-05	$\delta^{13}C = 0.74 \times (PET/P) - 34.8$	0.55	0.04
	2013-Sep-02		0.04	0.33